Robust active vibration control of piezoelectric flexible structures using deterministic and probabilistic analysis

Kai Zhang, Gérard Scorletti, Mohamed Ichchou, F. Mieyeville

Robust Active Vibration Control of Piezoelectric Flexible Structures using Deterministic and Probabilistic Analysis

K. Zhang

Laboratoire de Tribologie et Dynamique des Systèmes, Ecole Centrale de Lyon, 36 avenue Guy de Collongue,69134 Ecully Cedex,France

G. Scorletti

Laboratoire Ampère, Ecole Centrale de Lyon, 36 avenue Guy de Collongue,69134 Ecully Cedex,France

M.N. Ichchou*

Laboratoire de Tribologie et Dynamique des Systèmes, Ecole Centrale de Lyon, 36 avenue Guy de Collongue,69134 Ecully Cedex,France

F. Mieyeville

L'Institut des Nanotechnologies de Lyon, Ecole Centrale de Lyon, 36 avenue Guy de Collongue,69134 Ecully Cedex,France

Abstract

The main objective of this article is to propose a general and systematic robust control methodology for active vibration control of piezoelectric flexible structures such that the probabilistic information of parametric uncertainties can be investigated and the robustness properties of the closed-loop system can be quantitatively ensured. For the purpose, the modal parameter identification is performed based on the finite element analysis to have the reduced nominal dynamical models. The generalized polynomial chaos (gPC) framework is employed for uncertainty analysis to obtain the probabilistic informa-

*Corresponding author
Email address: mohamed.ichchou@ec-lyon.fr (M.N. Ichchou)

tion of parametric uncertainties. In the presence of probabilistic parametric and dynamic uncertainties, phase and gain control policies based H_∞ output feedback control is used for the controller design to ensure a set of control objectives simultaneously and then deterministic and probabilistic robustness analysis are conducted to quantitatively verify the robustness properties of the closed-loop system both in the deterministic sense and the probabilistic one. The design process and effectiveness of the proposed methodology are illustrated via active vibration control of a piezoelectric cantilever beam.
Keywords: H_∞ control, phase and gain control policies, probabilistic parametric uncertainties, gPC, μ/ν analysis, random algorithm

1. INTRODUCTION

Due to space and weight constrains, flexible structures are extensively used in many applications such as aerospace and automotive ones. The lightly damped nature of flexible structures can lead to considerable structural vibrations and cause unpleasant noises, unwanted stresses, malfunctions and even structural failures. In recent years, piezoelectric materials have been widely used as transducers for efficient active vibration control of various flexible structures (Garcia et al., 1992; Qiu and Tani, 1995; Jemai et al., 1999; Zhang et al., 2004). Owing to the complex dynamics of piezoelectric flexible structures, their dynamical models are normally obtained with finite element method (FEM) and/or system identification (Tzou and Tseng, 1990; Dong et al., 2006). However, in the presence of random variations in structural properties and/or the errors in the identification process, the obtained dynamical models inevitably have parametric uncertainties. Besides, a dynamic uncertainty is necessary to represent high-frequency neglected dynamics which may lead to the spill-over effect (Balas, 1978b,a). When

active control systems are designed based on the reduced nominal models, it is crucial to take into account different inaccuracies in these models to ensure the stability and the performance of the final closed-loop system. Considering the presence of parametric and dynamic uncertainties, phase and gain control policies based H_∞ output feedback control is proposed in Zhang et al. (2012), which affords a principle for the weighting function selection in H_∞ control to consider a set of control objectives simultaneously. However, this control method can only provide qualitative robustness properties of the closed-loop system. Furthermore, no probabilistic information of parametric uncertainties can be considered and thus every natural frequency is assumed to be independent parametric uncertainties and have uniform distribution within a given range. This assumption could be very conservative from a practical point of view. To overcome these problems, this article focuses on developing a general and systematic robust control methodology for active vibration control of piezoelectric flexible structures. It is expected to consider the probabilistic information of parametric uncertainties, *e.g.* the important natural frequencies, and to quantitatively verify the robustness properties of the closed-loop system both in the deterministic sense and the probabilistic one.

Considering structural complexity and manufacturing or measuring errors, structural properties of practical piezoelectric flexible structures usually have substantial levels of uncertainty, which may have considerable effects on the system natural frequencies. Furthermore, normally no analytical formulation of the natural frequencies is available for complex piezoelectric flexible structures. As a result, several numerical methods are proposed to investigate the effects of the structural property uncertainties on the natural frequencies and to achieve their distributions. This is usually referred to as

uncertainty propagation and Monte Carlo Simulation (MCS) (Liu, 2008) is a well-known technique in this field, with which the entire probability density function of any random variable can be computed, but the computation cost is usually expensive since a large number of samples are required for reasonable accuracy. The generalized polynomial chaos (gPC) framework is gaining in popularity and can be applied to various engineering problems (Ghanem and Spanos, 1991; Xiu and Karniadakis, 2002; Hou et al., 2006). It has been proved that gPC based uncertainty propagation methods are computationally far superior to traditional MCS methods (Xiu and Karniadakis, 2002). In Manan and Cooper (2010) and Kishor et al. (2011), Latin Hypercube Sampling (LHS) is employed in gPC framework to compute the polynomial chaos coefficients using the regression and variance analysis. To take into account probabilistic information of parametric uncertainties in the controller design, the probability theory is incorporated into classical robust and optimal control such as scenario approach based probabilistic robust control and probabilistic LQR design (Tempo et al., 2004). Besides, gPC framework is recently employed to solve this problem (Fisher and Bhattacharya, 2009; Duong and Lee, 2010; Templeton et al., 2012). The central idea and main interest of the gPC based probabilistic robust control is to substitute random variables into the original stochastic system by truncated polynomial chaos expansion according to their distributions. This generates a finite set of deterministic differential equations in a higher-dimensional space and estimates every original state $x_i(t, \Delta)$ with its truncated polynomial chaos expansion $\hat{x}_i(t)$.

In this article, the control problem is solved by building a bridge among multi-discipline techniques. Firstly, reduced nominal dynamical models are obtained with finite element analysis and modal parameter identification.

The gPC framework with LHS is used to propagate structural property uncertainties into the natural frequencies (Section 2). Then, in the presence of parametric and dynamic uncertainties, phase and gain control policies based H_∞ output feedback control is used for the controller design to satisfy a set of predetermined control objectives. With the designed controller, reliable deterministic and probabilistic robustness analysis are conducted with μ/ν analysis and random algorithm respectively (Zhou et al., 1996; Calafiore et al., 2000). They take into account the probabilistic information of parametric uncertainties and quantitatively verify the robustness properties both in the deterministic sense and the probabilistic one. Lastly, according to the results of the robustness analysis, if necessary, the weighting functions used in H_∞ controller can be retuned and a risk-adjusted trade-off could be made among various control objectives (Section 3).

Compared to the proposed control methodology, where phase and gain control policies based H_∞ output feedback control and reliable various robustness analysis are conducted separately, the μ synthesis such as widely used DK-iteration has some remarkable problems, *e.g.* the computational convergence and reliable estimation of μ upper bound for flexible structures. These problems indeed limit realistic use and effectiveness of μ synthesis (Skogestad and Postlethwaite, 2005). Moreover, the proposed control methodology avoids the estimation of state $x_i(t, \Delta)$, which is required by gPC based probabilistic robust control. Actually, this estimation is only suited in a limited short time and has no guaranteed accuracies. Additionally, no dynamic uncertainty can be represented with the gPC framework and thus it is impossible to apply gPC based control in the presence of a dynamic uncertainty. The computational cost of the gPC based control is also a problem in its practical application. With respect to the specifications of vibration

reduction normally defined in the frequency domain, neither gPC based control (Smith et al., 2006; Duong and Lee, 2010) nor probabilistic LQR is suitable in that they are mainly to design an optimal H_2 or LQR controller with state-feedback for minimizing a cost function or for the reference tracking specified in the time domain. These comparisons provide us confidence to believe that the proposed control methodology control is the most appropriate for efficient active vibration control of piezoelectric flexible structures, where the probabilistic information of parametric uncertainties is investigated and the robustness properties of the closed-loop system are quantitatively ensured both in the deterministic sense and the probabilistic one. To illustrate the design process of the proposed control methodology and evaluate its effectiveness, a numerical case study is conducted in Section 4. Conclusions and perspectives are summarized in Section 5.

2. SYSTEM ANALYSIS

As known, one of the most significant characteristics of flexible structures is their highly resonant modes due to inherently small dissipation of kinetic and strain energy as reflected by a relatively small structural damping. This means that such flexible structures may experience considerable vibrations when they are excited around the resonant frequencies. Therefore, active vibration control is desirable to effectively reduce the frequency response magnitudes caused by external disturbance. To achieve this goal, the deterministic system modeling and the uncertainty analysis are required before detailed controller design.

2.1. Deterministic System Modeling

Based on finite element modeling of piezoelectric flexible structures (Piefort, 2001), it is known that the plant transfer function $G_p(s)$ from the voltage

$V(s)$ exerted on one piezoelectric actuator to the acceleration output $\ddot{Y}(x_s, s)$ at location x_s has the form

$$G_p(s) = \frac{\ddot{Y}(x_s, s)}{V(s)} = \sum_{k=1}^{\infty} G_{pk}(s) = \sum_{k=1}^{\infty} \frac{R_k s^2}{s^2 + 2\zeta_k \omega_k s + \omega_k^2} \tag{1}$$

Similarly, the disturbance transfer function $G_d(s)$ from the external disturbance force $F(x_d, s)$ at location x_d to $\ddot{Y}(x_s, s)$ is

$$G_d(s) = \frac{\ddot{Y}(x_s, s)}{F(x_d, s)} = \sum_{k=1}^{\infty} G_{dk}(s) = \sum_{k=1}^{\infty} \frac{Q_k s^2}{s^2 + 2\zeta_k \omega_k s + \omega_k^2} \tag{2}$$

These models have an infinite number of resonant modes, however, in practice only the first few resonant modes can be employed in the controller design and the high-frequency neglected dynamics are represented by a dynamic uncertainty. To identify the modal parameters of $G_p(s)$ and $G_d(s)$, their frequency responses $T_{xy}(G_p(j\omega))$ and $T_{xy}(G_d(j\omega))$ can be computed with the commercial software COMSOL over interested frequency ranges. This can be regarded to be analogous to performing realistic experimental investigations (Dong et al., 2006). Then, best curve fitting is performed to have those modal parameters (Schoukens and Pintelon, 1991). It is notable that $G_p(s)$ and $G_d(s)$ should have the same natural frequencies despite the errors in the curve fitting.

2.2. Parametric Study

In this article, the generalized polynomial chaos (gPC) framework, *i.e.* Wiener-Askey polynomial chaos, is used to propagate structural property uncertainties into the natural frequency ω_k and to achieve its probabilistic information. According to the gPC framework, we have the correspondence between the choice of the distribution of random variable ξ and the orthogonal polynomials $\Gamma_i(\xi)$ as summarized in Table 1 (Xiu and Karniadakis, 2002).

For example, if Young's Modulus E of the flexible structure is assumed to have Gaussian distribution, *i.e.* $E \sim N(\mu_E, \sigma_E^2)$, 1−D Hermite polynomials can be used for ω_k

$$\omega_k = \beta_{0k} + \beta_{1k}\xi_1 + \beta_{2k}(\xi_1^2 - 1) + \beta_{3k}(\xi_1^3 - 3\xi_1) + \beta_{4k}(\xi_1^4 - 6\xi_1^2 + 3) + \dots \quad (3)$$

where $\xi_1 = \frac{E-\mu_E}{\sigma_E}$ is a normalized random variable. Similarly, to consider independent variables, *e.g.* the Young's Modulus $E \sim N(\mu_E, \sigma_E^2)$ and the density of the flexible structure $\rho \sim N(\mu_\rho, \sigma_\rho^2)$, 2−D Hermite polynomials can be used

$$\omega_k = \beta_{0k} + \beta_{1k}\xi_1 + \beta_{2k}\xi_2 + \beta_{3k}(\xi_1^2 - 1) + \beta_{4k}\xi_1\xi_2 + \beta_{5k}(\xi_2^2 - 1) + \dots \quad (4)$$

where $\xi_2 = \frac{\rho-\mu_\rho}{\sigma_\rho}$. The coefficients β can be determined using sampling scheme Latin Hypercube Sampling (LHS) with the regression and analysis of variance (Choi et al., 2004).

Random variable ξ	$\Gamma_i(\xi)$ of the Wiener-Askey scheme
Gaussian	Hermite
Uniform	Legendre
Gamma	Laguerre
Beta	Jacobi

Table 1: The correspondence between choice of the distribution of random variable ξ and polynomials $\Gamma_i(\xi)$ (Xiu and Karniadakis, 2002)

3. PROPOSED ROBUST CONTROL METHODOLOGY

3.1. Phase and Gain Control Policies Based H_∞ Output Feedback Control

Phase and gain control policies based H_∞ output feedback control is used for the controller design. The typical H_∞ control framework for active vibration control is shown in Figure 1, where G_p and G_d represent reduced

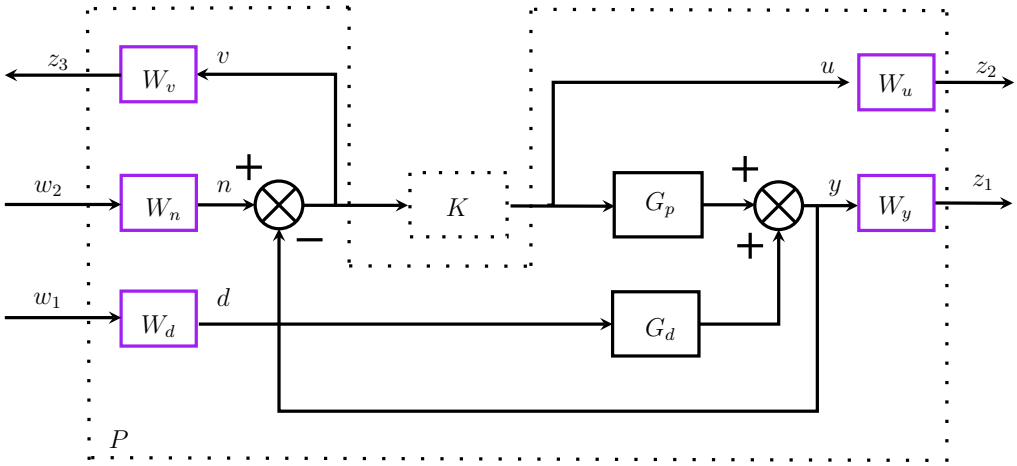

Figure 1: H_∞ control structure

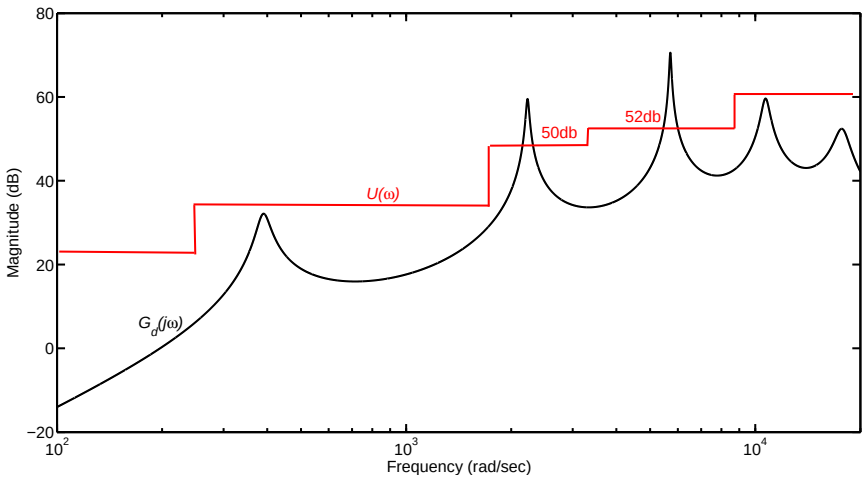

Figure 2: The specification of vibration control: $U(\omega)$

nominal plant and disturbance dynamical models respectively, K the controller to be designed, d the disturbance signal, n the measurement noise, y the output from the accelerometer, u the control energy, v the input signal to K. By incorporating weighting functions W_i, we have exogenous input signals w and regulated variable z. Appropriate selection of W_i is critical in H_∞ control to account for the relative magnitude of signals, their fre-

quency dependence and their relative importance. Phase and gain control policies can offer available guidelines for the selection of W_i according to the specification of vibration reduction for flexible structures, for example, as illustrated in Figure 2, where the modulus of the frequency response of the transfer function between the disturbance input and the system output must be smaller than a user defined frequency-dependant positive function $U(\omega)$. The details of phase and gain control policies based H_∞ output feedback control are presented in Zhang et al. (2012) and the principle of phase and gain control policies is emphasized below:

- Roughly speaking, when $|G_d(j\omega)| > U(\omega)$ the phase control policy has to be used such that the controller gain $|K(j\omega)|$ is large enough for the specification of vibration reduction. Meanwhile, the robust stability to parametric uncertainties such as ω_k and ζ_k is qualitatively guaranteed by constraining the stable open loop transfer function $L(j\omega) = G_p(j\omega)K(j\omega)$ to stay in the right half plane (RHP) on Nyquist plot around the controlled resonant frequencies, that is, $\mathrm{Re}(L(j\omega)) \geq 0,\ \omega \in [\omega_k - \delta_{\omega_k},\ \omega_k + \delta_{\omega_k}]$. This can be regarded as a generalization of the passivity theorem (Khalil, 1996) based active vibration control, where collocated senors and actuators are required to guarantee the positive-realness of $G_p(j\omega)$ (Zhou et al., 1996; Friswell et al., 1997; Moheimani and Vautier, 2005; Demetriou et al., 2009; Jiang and Li, 2011). By taking advantages of the positive-realness of $G_p(j\omega)$, a strictly positive real stable controller $K(j\omega)$, *e.g.* the velocity feedback controller (Balas, 1979), can be used to ensure $L(j\omega)$ positive real. For instance, for single-input and single-output (SISO) systems, the positive real $L(j\omega)$ implies that $L(j\omega)$ retains in RHP at any frequency, *i.e.* $\mathrm{Re}(L(j\omega)) \geq 0,\ \forall\omega$. This ensures that the closed-loop stability can

be unconditionally satisfied in the presence of any level of parametric and dynamic uncertainties only if $L(j\omega)$ keeps positive real. However, sometimes due to the physical limitations or to have better control efficiency, a non-collocated control system has to be employed, which makes $G_p(j\omega)$ ($L(j\omega)$) have no positive-realness. Furthermore, even the positive-realness of $G_p(j\omega)$ is guaranteed by collocated sensors and actuators, a non positive real controller, *e.g.* the acceleration feedback control (Bayon de Noyer and Hanagud, 1998), may be used to make a trade-off between the stability robustness and other control objectives. The non-positive real $L(j\omega)$ poses challenging problems for the controller design proposed for collocated systems. In such cases the phase control policy is desirable to employ.

- When $|G_d(j\omega)| \leq U(\omega)$ no control energy is needed and the gain control policy is used to make $|K(j\omega)|$ as small as possible to limit the control energy and have certain robust stability to the dynamic uncertainty based on the small gain theorem (Desoer and Vidyasagar, 1975). Actually the gain control policy can represent not only usual high-frequency neglected dynamics but may also include the dynamics over low or middle frequency ranges, where the phase control policy is not used. This means that the control energy is only advertently supplied to the controlled resonant modes.

Applying phase and gain control policies to H_∞ control, a set of weighting functions can be appropriately determined such that all the predetermined control objectives are satisfied simultaneously.

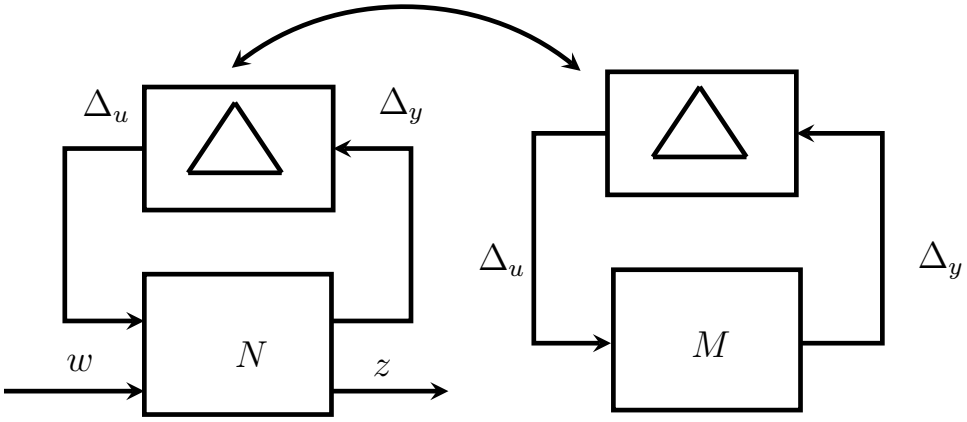

Figure 3: General LFT framework

3.2. Deterministic and Probabilistic Robustness Analysis

Although phase and gain control policies based H_∞ control qualitatively account for parametric and dynamic uncertainties, it is desirable to perform deterministic and probabilistic robustness analysis to consider probabilistic information of parametric uncertainties and quantitatively ensure robustness properties of the closed-loop system both in the deterministic sense and the probabilistic one.

3.2.1. Deterministic robustness analysis

To perform deterministic robustness analysis, the original stochastic system with parametric and dynamic uncertainties has to be rearranged by the uncertainty block Δ and nominal augmented plant N as shown in Figure 3 (Zhou et al., 1996), where $w(s)$ consists of exogenous input signals and $z(s)$ consists of regulated variables. N can always be chosen so that Δ is block diagonal, that is, $\Delta \in \mathbf{\Delta}$

$$\mathbf{\Delta} \triangleq \{\text{diag}\,[\delta_1^r I_{t_1}, \ldots, \delta_V^r I_{t_V}, \delta_{V+1}^c I_{r_1}, \ldots, \delta_{V+S}^c I_{r_S}, \Delta_{V+S+1}, \ldots, \Delta_{V+S+F}] :$$
$$\delta_k^r \in \mathbb{R},\ \delta_{V+i}^c \in \mathbb{C},\ \Delta_{V+S+j} \in \mathbb{C}^{m_j \times m_j}, 1 \le k \le V,\ 1 \le i \le S, 1 \le j \le F\}$$

where $\mathbb{R}$ and $\mathbb{C}$ denote the fields of real and complex numbers, δ_k^r represents the k^{th} real scale parametric uncertainty with t_k repetition, δ_{V+i}^c represents the i^{th} repeated complex scalar uncertainty with r_i repetition and Δ_{V+S+j} represents the j^{th} full dynamic uncertainty with size $m_j \times m_j$. By incorporating suitable normalization functions in N such as $W_{\text{Dyn}}(j\omega)$ for the dynamic uncertainty, we have $\delta_k^r \in [-1, 1]$, $|\delta_i^c| \leq 1$ and $\bar{\sigma}(\Delta_j) \leq 1$ and the notation $\boldsymbol{B}_\Delta$ is introduced for the norm bounded diagonal uncertainty block

$$\boldsymbol{B}_\Delta := \{\Delta \in \boldsymbol{\Delta} : \ \bar{\sigma}(\boldsymbol{\Delta}) \leq 1\}$$

By partitioning $N(s)$ compatibly with the dimension of $\Delta(s)$ we have

$$\begin{bmatrix} \Delta y \\ z \end{bmatrix} = \begin{bmatrix} N_{11} & N_{12} \\ N_{21} & N_{22} \end{bmatrix} \begin{bmatrix} \Delta u \\ w \end{bmatrix} ; \ M = N_{11} \tag{5}$$

The closed-loop transfer function from $w(s)$ to $z(s)$ is represented by an upper linear fractional transformation (LFT), $\mathscr{F}_u(N, \Delta)$,

$$z(s) = \mathscr{F}_u(N, \Delta)w(s) = (N_{22} + N_{21}\Delta(I - N_{11}\Delta)^{-1}N_{12})w(s) \tag{6}$$

Based on general LFT framework, the structured singular value $\mu_\Delta(M)$ is defined (Skogestad and Postlethwaite, 2005)

$$\mu_\Delta(M) \triangleq \frac{1}{\min\{k_m | \ \det(I - k_m M\Delta) = 0, \ \Delta \in \boldsymbol{B}_\Delta\}} \tag{7}$$

The closed-loop robust stability is then determined by the following theorem (Zhou et al., 1996)

Theorem 3.1. *Assume that the nominal system M and the perturbation Δ are stable. Then the $M - \Delta$ is stable for any $\Delta \in \boldsymbol{B}_\Delta$ if and only if*

$$\mu_\Delta(M(j\omega)) < 1, \ \forall\omega \tag{8}$$

Besides robust stability, the worst-case performance of the closed-loop system has to be investigated. Let us denote $\Delta_1 = \text{diag}(\Delta_{\text{Para}},\ \Delta_{\text{Dyn}}) \in \boldsymbol{B}_{\Delta_1}$ and define the worst-case performance λ_{wc} as

$$\lambda_{wc}(\omega) \triangleq \sup_{\Delta_1 \in \boldsymbol{B}_{\Delta_1}} \bar{\sigma}(\mathscr{F}_u(N, \Delta_1)(j\omega)),\ \forall\omega \tag{9}$$

then skewed μ (ν) analysis is performed using a norm bounded fictitious performance uncertainty $\Delta_2 = \Delta_{\text{Perf}}(j\omega)$, *i.e.* $\bar{\sigma}(\Delta_2) \leq 1$, and a corresponding performance normalization function $W_{\text{Perf}}(j\omega) = \frac{1}{U(\omega)}$. According to the definition of $\nu(\hat{N})$ (Ferreres and Fromion, 1999)

$$\nu(\hat{N}) \triangleq \frac{1}{\min\{k_n |\ \det(I - k_n\hat{N}\Delta) = 0,\ \Delta = \text{diag}(\Delta_1,\ k_n\Delta_2),\ \Delta_i \in \boldsymbol{B}_\Delta\}} \tag{10}$$

we have

$$\nu(\hat{N}(j\omega)) \leq 1 \Leftrightarrow \lambda_{wc}(\omega) \leq U(\omega), \forall\omega \tag{11}$$

Compared to original N in Equation (5) for classical μ analysis, $\hat{N}$ also incorporates $W_{\text{Perf}}(j\omega)$. In addition, with ν analysis we can calculate the largest gain $\gamma_{\text{perf}}(\omega)$, which represents how much the normalized parametric and dynamic uncertainties can be enlarged simultaneously before the worst-case performance is violated,

$$\gamma_{\text{perf}}(\omega) \triangleq \sup_{\gamma} \sup_{\Delta_1 \in \gamma\boldsymbol{B}_{\Delta_1}} \bar{\sigma}(\mathscr{F}_u(N, \Delta_1)(j\omega)) \leq U(\omega), \forall\omega \tag{12}$$

As $U(\omega)$ is a frequency dependent function, $\gamma_{\text{perf}}(\omega)$ also depends on ω. In the following γ_{perf} is used for the sake of simplicity.

As accurate calculation of the value of $\mu_\Delta(M)$ is NP-hard (Braatz et al., 1994), lower and upper bounds of $\mu_\Delta(M)$ are usually computed. The reciprocal of upper bound of $\mu_\Delta(M)$ is referred to as deterministic robustness margin

$$k_{\text{DRM}} = \frac{1}{\max \mu_\Delta(M)} \tag{13}$$

It means how much the normalized parametric and dynamic uncertainties can be enlarged simultaneously before the closed-loop system gets instable. The lower bound of $\mu_\Delta(M)$ provides a destabilizing perturbation and reflects the conservatism in the upper bound. To compute the upper and lower bounds of $\mu_\Delta(M)$, Matlab Robust Control Toolbox makes use of the results from Young and Dolye (1990) and Young et al. (1992), where the frequency gridding is used over frequency ranges of interest. However, in the case of lightly damped flexible systems, narrow and high peaks on $\mu_\Delta(M(j\omega))$ plot commonly exist around resonant frequencies (Freudenberg and Morton, 1992). This implies that if the frequency gridding is not sufficient enough and neglects the critical frequency at which $\mu_\Delta(M(j\omega))$ is maximal, the robustness properties are overestimated. Therefore, in this article besides the ordinary frequency gridding method as used in Iorga et al. (2009), a frequency interval method (Ferreres et al., 2003) is applied to have more reliable results, *i.e.* they are neither conservative nor overestimated. Similarly, for reliable $\nu(\hat{N})$ calculation for lightly damped flexible systems, both Matlab built-in function 'wcgain' and the general skewed mu toolbox (SMT) (Ferreres et al., 2004) can be used, which employs the frequency gridding method and the frequency interval method respectively.

3.2.2. Probabilistic robustness analysis

In the context of probabilistic robustness analysis, the uncertainty Δ is indeed bounded within a given set but it is also a random matrix with support $\mathcal{B}_{\mathbb{D}}(\rho) = \{\Delta : \Delta \in \rho \boldsymbol{B}_\Delta\}$ having given distribution (Tempo et al., 2004). In this article, probabilistic robustness margin k_{PRM} and probabilistic worst-case performance are computed with a randomized algorithm such as Monte Carlo Simulation (MCS).

Based on an associated positive level γ, the probability of k_{PRM} is repre-

sented by $p(\gamma)$ defined as

$$p(\gamma) \triangleq P_R\{k_{\text{PRM}} \leq \gamma\} \tag{14}$$

This means that with probability $p(\gamma)$, we have $k_{\text{PRM}} \leq \gamma$. As exact computation of $p(\gamma)$ is in general very difficult, $p(\gamma)$ is usually estimated by its empirical probability $\hat{p}_N(\gamma)$. For every value of γ, the random sampling generates the uncertainties as $\Delta^1, \Delta^2, \ldots, \Delta^n \in \mathcal{B}_{\mathbb{D}}(\gamma)$ and thus $\hat{p}_n(\gamma)$ is

$$\hat{p}_n(\gamma) = \frac{1}{n}\sum_{i=1}^{n} I(\Delta^i),\ \Delta^i \in \mathcal{B}_{\mathbb{D}}(\gamma) \tag{15}$$

where $I(\Delta^i)$ is a indicator to the stability of the closed-loop system: $I(\Delta^i) = 1$ means the closed-loop system is stable, otherwise, $I(\Delta^i) = 0$. The sampling number n is based on Chernoff bound (Tempo et al., 1997), that is, for any $\epsilon \in (0, 1)$ and $\delta \in (0, 1)$,

$$n \geq \frac{1}{2\epsilon^2}\log\frac{2}{\delta} \tag{16}$$

Obviously, this sampling number n is independent on the number of uncertainties. It ensures that with the probability $1 - \delta$, we have

$$|\hat{p}_n(\gamma) - p(\gamma)| \leq \epsilon.$$

To perform probabilistic worst-case performance for the specification of vibration reduction, denote $J(\Delta^i) = \bar{\sigma}(\mathscr{F}_u(N, \Delta^i)(j\omega)),\ \forall\omega$ and define $\lambda_{wc}(\rho)$ for every interested ρ,

$$\lambda_{wc}(\rho) \triangleq \sup_{\Delta^i \in \mathcal{B}_{\mathbb{D}}(\rho)} (J(\Delta^i)) \tag{17}$$

As exact computation of $\lambda_{wc}(\rho)$ is very difficult, it is usually estimated by its empirical probability $\bar{\lambda}_m(\rho)$ defined as

$$\bar{\lambda}_m(\rho) = \max_{\substack{\Delta^i \in \mathcal{B}_{\mathbb{D}}(\rho),\\ i=1,2\ldots,m}} J(\Delta^i) \tag{18}$$

where the uncertainties $\Delta^1, \Delta^2, \ldots, \Delta^m \in \mathcal{B}_{\mathbb{D}}(\rho)$ are randomly generated and the sampling number m is determined based on log-over-log bound (Tempo et al., 1997), that is, for any $\epsilon \in (0,1)$ and $\delta \in (0,1)$,

$$m \geq \frac{\log \frac{1}{\delta}}{\log \frac{1}{1-\epsilon}} \tag{19}$$

This sampling number m ensures that with the probability $1-\delta$, we have

$$P_R\{\lambda_{wc}(\rho) > \bar{\lambda}_m(\rho)\} \leq \epsilon.$$

From the definition of γ_{perf} in Equation (12), ρ can be regarded as risked adjusted $\tilde{\gamma}_{\text{perf}}$ in a probabilistic sense.

With given $\epsilon \in (0,1)$ and $\delta \in (0,1)$, the focus of probabilistic robustness analysis is to compute $\hat{p}_n(\gamma)$ and $\bar{\lambda}_m(\rho)$ for interested γ and ρ, which are associated with k_{PRM} and $\tilde{\gamma}_{\text{perf}}$. On the one hand, k_{PRM} and $\tilde{\gamma}_{\text{perf}}$ can be used to verify the conservatism and the overestimation in k_{DRM} and γ_{perf} in a nearly deterministic sense. On the other hand, they can be used to reflect the conservatism in k_{DRM} and γ_{perf} to some extent in a probabilistic sense. Obviously, above deterministic and probabilistic robustness analysis complement and compare each other and can provide reliable and comprehensive investigation of the closed-loop robustness properties.

4. NUMERICAL CASE STUDY

The design process and effectiveness of the proposed control methodology are illustrated by robust active vibration control of the piezoelectric cantilever beam consisting of one piezoelectric actuator and one accelerometer as shown in Figure 4. With nominal structural properties, finite element analysis (FEA) is performed in COMSOL and then parameter identification is used to acquire the corresponding plant and dynamical models $G_p(s)$ and

$G_d(s)$ with the first five resonant modes. Their frequency responses are well consistent with those from FEA as shown in Figure 5. As expected, the poles are the same for $G_p(s)$ and $G_d(s)$.

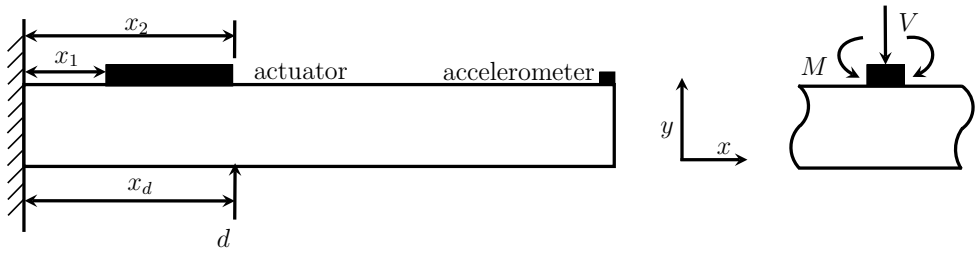

Figure 4: The piezoelectric cantilever beam

According to the specification of vibration reduce illustrated in Figure 2 and the principle of phase and gain control polices, only the first three resonant modes are necessary to employ in H_∞ control and thus the effects of structural properties on $\omega_i,\ i = 1, 2, 3$ have to investigated. Other higher resonant modes are represented by a dynamic uncertainty. In this article, E and ρ of the cantilever beam are assumed to have Gaussian distributions, that is, $E \sim N(\mu_E, \sigma_E^2)$ and $\rho \sim N(\mu_\rho, \sigma_\rho^2)$ with $\mu_E = 50$ Gpa, $\sigma_E = 1.67$ Gpa and $\mu_\rho = 2500$ kg/m^3, $\sigma_\rho = 250$ kg/m^3. If only uncertain E is considered, with gPC framework and eigenvalues analysis in COMSOL, $1-$D PCE models are developed using 30 LHS and 10000 MCS samples, for example,

$$\begin{aligned} \omega_1 &= 219.0 + 3.46E;\ \text{MCS} \\ \omega_1 &= 219.2 + 3.46E;\ \text{PCE} \end{aligned}$$

Similarly when both uncertain E and ρ are investigated we have

$$\begin{aligned} \omega_1 &= 418.2 + 3.49E - 0.0798\rho;\ \text{MCS} \\ \omega_1 &= 414.2 + 3.45E - 0.0773\rho;\ \text{PCE} \end{aligned}$$

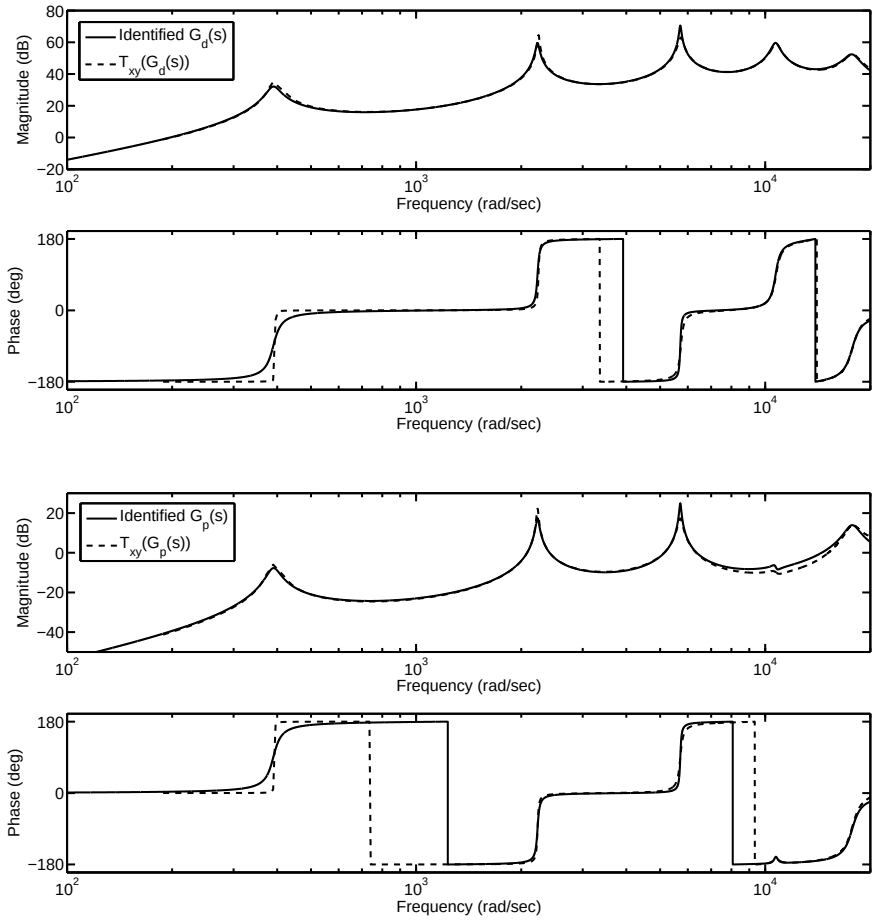

Figure 5: FEA and identified frequency responses of $G_d(s)$ and $G_p(s)$

where the units of ω and E are rad/sec and Gpa. This approximated linear relationship can also be explained from Taylor series expansions of theoretical ω_k without considering the effects of piezoelectric actuators (Qiu et al., 2009), that is, $\omega_k = g_k\sqrt{\frac{E}{\rho}}$, where g_k is an constant associated to structural properties. With the first-order Taylor series expansions for E, we have the comparisons of Figure 6, which demonstrate that gPC based uncertainty analysis have sufficient accuracy and great improvement in efficiency compared to MCS. It is also shown that for this particular case the effects of the bounded piezoelectric actuator on ω_k are significant and must be taken

into account in the system modeling. This is different from the case in Qiu et al. (2009). As ω_k is more sensitive to the variation of E compared to that of ρ, for the sake of simplicity, only uncertain E is considered in subsequent robustness analysis.

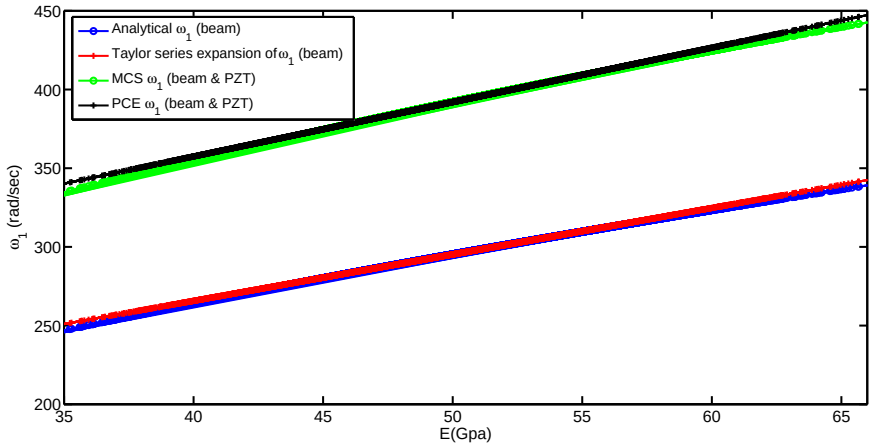

Figure 6: Theoretical, Taylor series expansion, MCS and PCE for ω_1

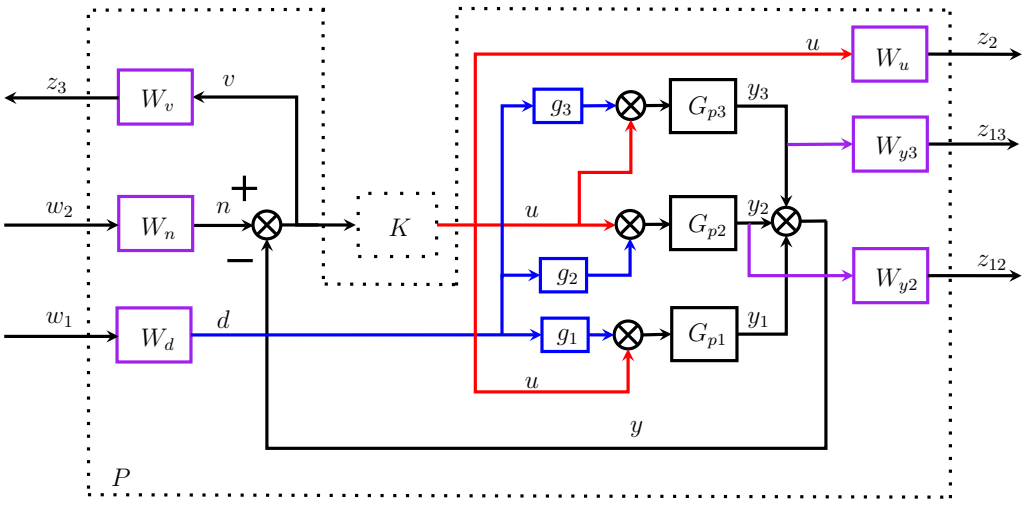

Figure 7: The decomposed H_∞ control structure

In the H_∞ controller design and the robustness analysis, the relation-

ship between $G_{dk}(s)$ and $G_{pk}(s)$ is considered with the scale constant g_k as illustrated in the decomposed H_∞ control structure of Figure 7. This decomposition can reduce the achieved H_∞ controller order and allow us to make a trade-off among the vibration reduction for every controlled mode. When the phase control policies is used $L(j\omega)$ has to be large enough and $|K(j\omega)(1+L(j\omega))^{-1}| \approx |K(j\omega)|$. This implies that the requirements on $|K(j\omega)|$ can be approximately reflected by $\|T_{w_2 \to z_2}(j\omega)\|_\infty \leq 1$, *i.e.* $|K(j\omega)| \leq \frac{1}{|W_n(s)W_u(s)|}$. Normally the larger $|K(j\omega)|$ is, the better the control performance is, however, this could degrade the robust stability of the closed-loop system in the presence of parametric and dynamic uncertainties and increase the control effort (Balas and Doyle, 1994). As a result, trade-offs among those control objectives have to be considered in the selection of W_i. In this particular case, it is apparent from Figure 2 that the phase control policy has to be applied to the second and third resonant modes and the gain control policy has to be applied to the first resonant mode and high-frequency neglected ones. Therefore, a second order $W_u(s)$ is used

$$W_u(s) = k\frac{s + M\omega_B^*}{s + \epsilon}\frac{s + fM\omega_B^*}{s + 0.1fM^2\omega_B^*} \tag{20}$$

where the parameters $k,\ \epsilon,\ M,\ f$ and ω_B^* are determined based on phase and gain control policies such that the requirements on $|K(j\omega)|$ are satisfied among different frequency ranges.

The following set of W_i is employed for this case: $W_n = 5, W_v = \frac{1}{50}, W_d = \frac{1}{100}, W_{y2} = \frac{1}{3.2}, W_{y3} = \frac{1}{4.0}$ and $k = 1,\ \epsilon = 10^{-6},\ M = 1000,\ f = 2,\ \omega_B^* = 3$. With these weighting functions, we have the corresponding controller $K_\infty(s)$. As expected and illustrated in Figure 8, with $K_\infty(s)$ the phase control policy is applied to the second and third resonant modes, *i.e.* around $\omega_{2/3}$ $|K_\infty(j\omega)|$ is large enough and $L(j\omega) = G_p(j\omega)K_\infty(j\omega)$ stays in RHP; the gain control policy is applied to the first resonant mode and high-frequency neglected

ones, *i.e.* around ω_1 $|K_\infty(j\omega)|$ is small and at high frequencies $K_\infty(j\omega)$ rolls off quickly, which ensures $|L(j\omega)|$ small enough at these frequencies. Although these analysis imply that with $K_\infty(s)$ qualitative robustness properties of the closed-loop system can be achieved, reliable robustness analysis has to be performed subsequently to obtain quantitative robustness properties.

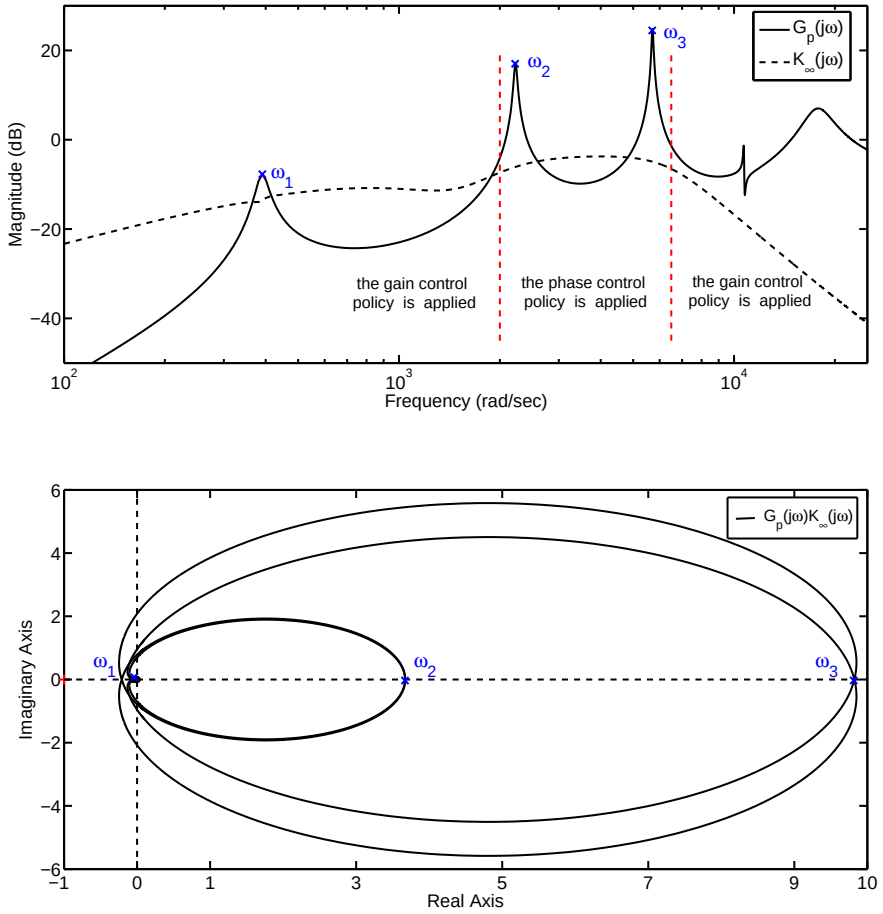

Figure 8: Phase and gain control polices with $K_\infty(s)$

Based on above uncertainty analysis with PCE, assuming $E \in [45, 55] = 50 + 5\delta_E,\ |\delta_E| \leq 1$, we have

$$\omega_k = \omega_{k0} + \omega_{k1}\delta_E;\ |\delta_E| \leq 1, k = 1, 2, 3$$

This transformation from δ_{ω_k} to δ_E allows us to consider the probabilistic information of ω_k due to distributed E and the relationship among every ω_k. Uncertain ζ_k can be assumed to have certain deviation such as 20% about its nominal value

$$\zeta_k = \zeta_{k0} + \zeta_{k1}\delta_{\zeta_k};\ |\delta_{\zeta_k}| \leq 1, \zeta_{k1} = 0.2\zeta_{k0}, k = 1, 2, 3$$

To represent dynamic and fictitious performance uncertainties, norm bounded uncertainty $\Delta_{\text{Dyn}}(j\omega)$ and $\Delta_{\text{Perf}}(j\omega)$ are used with suitable dynamic normalization functions $W_{\text{Dyn}}(j\omega)$ and $W_{\text{Perf}}(j\omega)$. With Simulink modeling, the fact that $G_p(s)$ and $G_d(s)$ have the same natural frequencies is considered and the nominal augmented plant N' and corresponding structured uncertainty $\Delta' = \text{diag}(\Delta'_1,\ \Delta'_2) \in \boldsymbol{B}_\Delta$ are developed, where $\Delta'_1 = \text{diag}(\Delta_{\text{Para}},\ \Delta_{\text{Dyn}})$ and $\Delta'_2 = \Delta_{\text{Perf}}$, especially, $\Delta_{\text{Para}} = \text{diag}\ [\delta_E I_6, \delta_{\zeta 1}, \delta_{\zeta 2}, \delta_{\zeta 3}]$.

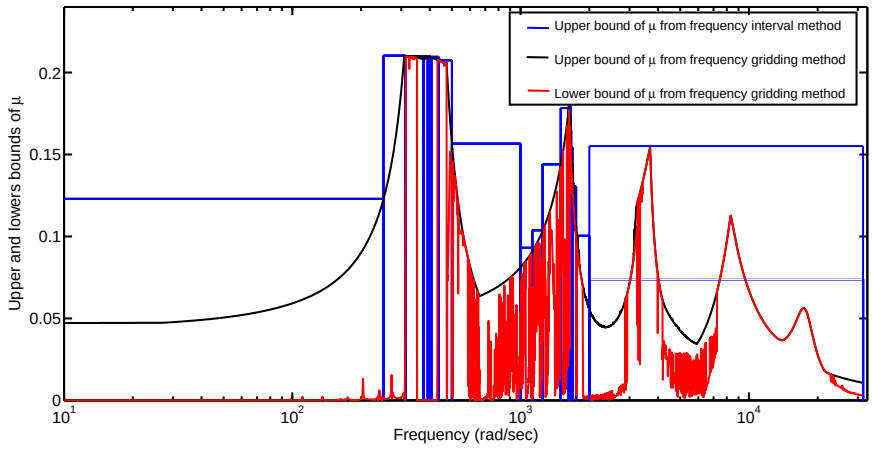

Figure 9: Deterministic robust stability analysis with $\zeta_{k1} = 0.2\zeta_{k0}$

With obtained N' and Δ', above mentioned frequency gridding and frequency interval methods are used for deterministic robustness analysis without considering any probabilistic information of ω_k or ζ_k. When $\zeta_{k1} = 0.2\zeta_{k0}$ the deterministic robust stability analysis of Figure 9 shows that the upper

and lower bounds of μ from the frequency gridding method coincide around resonant frequencies and they are also consistent well with the upper bound of μ from the frequency interval method. This means that the estimated μ and corresponding $k_{\mathrm{DRM}} = 4.76$ are reliable, in other words, the closed-loop system remains stable for any $\Delta \in 4.76\Delta_1'$. With ν analysis the results of deterministic worst-case performance are illustrated in Figure 10, which show that the upper and lower bounds of the worst-case performance from the frequency gridding method ('wcgain') coincide and they are also well consistent with the results from the frequency interval method (SMT). These results ensure that obtained $\gamma_{\mathrm{perf}} = 1.70$ is reliable, that is, the specification of vibration reduction is fulfilled for any $\Delta \in 1.70\Delta_1'$. It is notable that as every ω_k depends on δ_E, the worst-case performances for the second and third resonant modes can not happen at the same time.

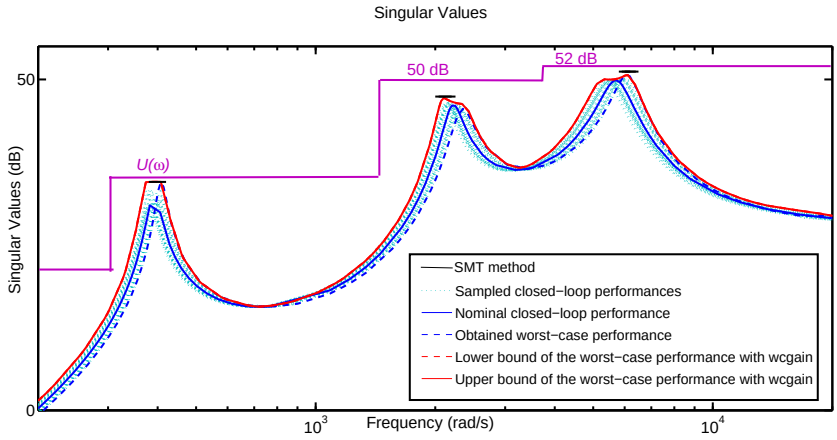

Figure 10: Deterministic worst-case performance with $\zeta_{k1} = 0.2\zeta_{k0}$ and $\Delta \in 1.70\Delta_1'$

Probabilistic robustness analysis is performed to consider probabilistic information of ω_k and ζ_k and provide complements and comparisons to above deterministic robustness analysis. In this numerical case, both uniformly and Gaussian distributed E are considered and ζ_k is assumed to have uni-

Uniformly distributed E	Gaussian distributed E
$\hat{p}_n(4.76) = 100\%$	$\hat{p}_n(4.76) = 100\%$
$\hat{p}_n(4.98) = 98.20\%$	$\hat{p}_n(4.98) = 98.22\%$

Table 2: Probabilistic stability analysis: $\epsilon = 0.01, \delta = 0.02, \zeta_{k1} = 0.2\zeta_{k0}$

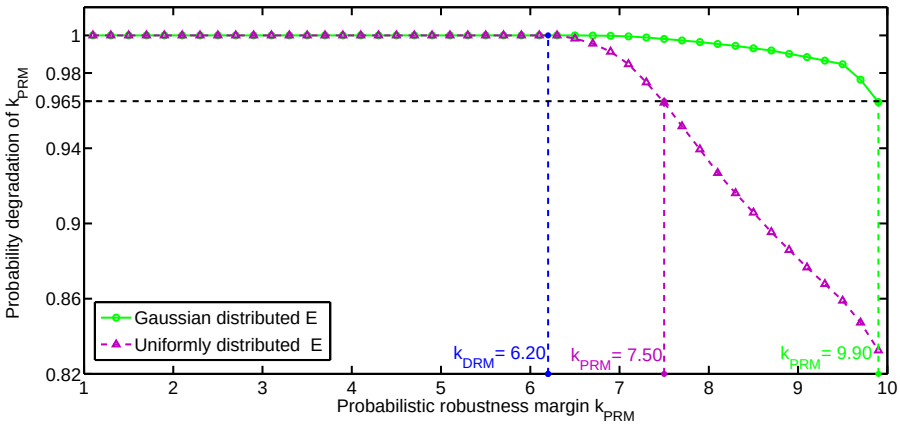

Figure 11: Probabilistic robust stability analysis with $\zeta_{k1} = 0.1\zeta_{k0}, \epsilon = 0.01, \delta = 0.02$

form distribution. When $\zeta_{k1} = 0.2\zeta_{k0}$ the results from probabilistic stability analysis are illustrated in Table 2 with $\epsilon = 0.01, \delta = 0.02$. It verifies that with probability $1 - \delta = 98\%$ for either uniformly or Gaussian distributed ω_k, the closed-loop system remains stable for all sampled $\Delta \in 4.76\Delta_1'$. Additionally, a few destabilizing perturbations $\Delta_{\text{des}} \in 4.77\Delta_1'$ are founded. It is reasonable to conclude that $k_{\text{DRM}} = 4.76$ from μ analysis is neither conservative nor overestimated. Probabilistic stability analysis also shows that for uniformly distributed E if a 1.80% loss of probabilistic robust stability is tolerated, the corresponding $k_{\text{PRM}} = 4.98$ is increased by 5.96% with respect to its deterministic counterpart $k_{\text{DRM}} = 4.76$.

Above probabilistic stability analysis is based on the normalization $\zeta_{k1} = 0.2\zeta_{k0}$, *i.e.* ζ_k have 20% deviation of its nominal value. This limits k_{DRM} and k_{PRM} smaller than 5 to guarantee $\zeta_k > 0$ and explains why this is no

significant difference between $k_{\mathrm{DRM}} = 4.76$ and $k_{\mathrm{PRM}} = 4.98$. To more clearly reveal the conservatism of k_{DRM} from a probabilistic point of view, ζ_k is assumed to have 10% deviation of its nominal value, *i.e.* $\zeta_{k1} = 0.1\zeta_{k0}$, but the normalization of other uncertainties are not changed. This enlarges allowable k_{DRM} and k_{PRM} to 10 and reduces the relative normalization of ζ_k with respect to that of other uncertainties as illustrated by red rectangles in Figure 12. When $\zeta_{k1} = 0.1\zeta_{k0}$, we have $k_{\mathrm{DRM}} = 6.20$ and the probability degradation function of k_{PRM} of Figure 11. This shows that with probability 98%, if a 3.50% loss of probabilistic robust stability is tolerated, for Gaussian distributed E $k_{\mathrm{PRM}} = 9.9$, which is increased by 59.7% with respect to its deterministic counterpart $k_{\mathrm{DRM}} = 6.20$ and increased by 32.0% with respect to the result for uniformly distributed E. The results are summarized in Table 3. Compared to Table 2, the difference between k_{DRM} and k_{PRM} is more significant. With this normalization, we have $\gamma_{\mathrm{perf}} = 2.0$. The effects of relative normalization of ζ_k with respect to that of other uncertainties on k_{DRM} and γ_{perf} are illustrated in Figure 12, where the zero point corresponds to the nominal values of the uncertainties.

Uniformly distributed E	Gaussian distributed E
$\hat{p}_n(6.20) = 100\%$	$\hat{p}_n(6.20) = 100\%$
$\hat{p}_n(7.50) = 96.5\%$	$\hat{p}_n(9.90) = 96.5\%$

Table 3: Probabilistic stability analysis: $\epsilon = 0.01$,$\delta = 0.02, \zeta_{k1} = 0.1\zeta_{k0}$

Probabilistic worst-case performance analysis is also performed. When $\zeta_{k1} = 0.2\zeta_{k0}$, the results are summarized in Table 4 and Table 5. On the one hand, from Table 4 it is demonstrated that with probability 98%, the specification of vibration reduction is fulfilled for all sampled $\Delta_1' \in 1.70\boldsymbol{B}_{\Delta_1}$, but when $\Delta_1' \in 1.72\boldsymbol{B}_{\Delta_1}$ a few perturbations can be founded to violate the specification of vibration reduction for uniformly distributed E. These re-

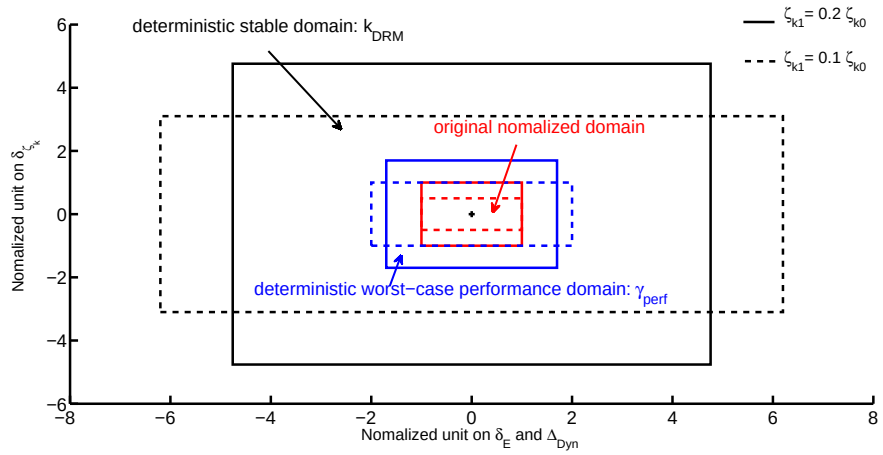

Figure 12: Deterministic robust domains in the space of uncertainties

sults verify that $\gamma_{\text{perf}} = 1.70$ from ν calculation is neither conservative nor overestimated. On the other hand, from Table 5 it is demonstrated that with probability 90%, the risk adjusted $\tilde{\gamma}_{\text{perf}} = 2.21$ for Gaussian distributed E. This is increased by 30.0% with respect to its deterministic counterpart $\gamma_{\text{perf}} = 1.70$ and increased by 15.1% with respect to the result for uniformly distributed E. The effects of various distributed E on the worst-case performance are also of significance in statistics meaning as illustrated in Figure 13 with $\epsilon = 0.001, \delta = 0.1, \zeta_{k1} = 0.2\zeta_{k0}$ and $\Delta_1' \in 2.10\boldsymbol{B}_{\Delta_1}$.

Targeted resonant mode	Uniformly distributed E	Gaussian distributed E
The second mode	$\bar{\lambda}_m(1.70) = 48.30\text{dB} < 50.00\text{dB}$ $\bar{\lambda}_m(1.72) = 49.04\text{dB} < 50.00\text{dB}$	$\bar{\lambda}_m(1.70) = 48.02\text{dB} < 50.00\text{dB}$ $\bar{\lambda}_m(1.72) = 48.70\text{dB} < 50.00\text{dB}$
The third mode	$\bar{\lambda}_m(1.70) = 51.67\text{dB} < 52.00\text{dB}$ $\bar{\lambda}_m(1.72) = 52.50\text{dB} > 52.00\text{dB}$	$\bar{\lambda}_m(1.70) = 51.50\text{dB} < 52.00\text{dB}$ $\bar{\lambda}_m(1.72) = 51.94\text{dB} < 52.00\text{dB}$

Table 4: Probabilistic worst-case performance analysis: $\epsilon = 0.001, \delta = 0.02, \zeta_{k1} = 0.2\zeta_{k0}$

Above deterministic and probabilistic robustness analysis show that for lightly damped flexible systems employed methods provide reliable calculation of μ and ν and thus we have neither conservative nor overestimated k_{DRM} and γ_{perf} in a deterministic sense, but these values may turn out to be

Targeted resonant mode	Uniformly distributed E	Gaussian distributed E
The second mode	$\bar{\lambda}_m(1.92) = 48.72$dB	$\bar{\lambda}_m(2.21) = 48.83$dB
The third mode	$\bar{\lambda}_m(1.92) = 52.00$dB	$\bar{\lambda}_m(2.21) = 52.00$dB

Table 5: Probabilistic worst-case performance analysis: $\epsilon = 0.001, \delta = 0.1, \zeta_{k1} = 0.2\zeta_{k0}$

conservative to some extent in a probabilistic sense as compared to k_{PRM} and $\tilde{\gamma}_{\text{perf}}$. These robustness analysis also demonstrate that with proposed control methodology we can have attractive robustness properties of the closed-loop system both in the deterministic sense and the probabilistic one. However, it is notable that the main purpose of the proposed control methodology is not only to design a good controller for active vibration control, which is sometimes easy to achieve with simpler control methods such as the velocity feedback control, the acceleration feedback control and so on, but also to offer a general and systematic way to achieve several trade-offs between conflicting objectives, *e.g.* the robust stability and robust performance, the vibration reduction for every targeted resonant mode and the deterministic and probabilistic robustness properties.

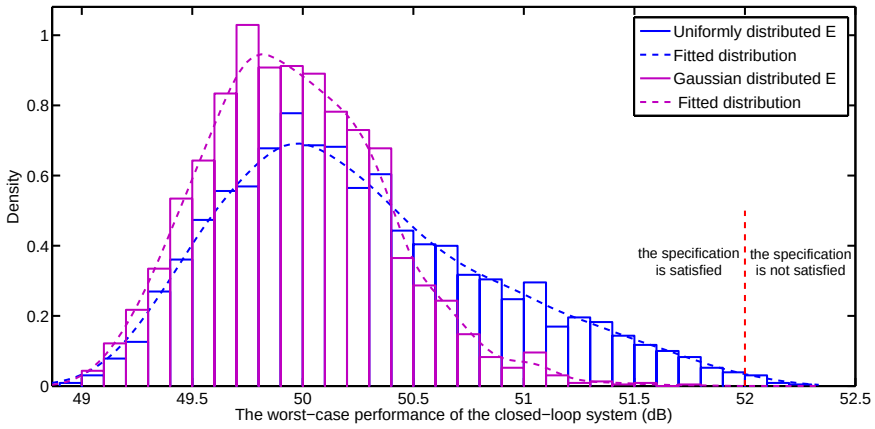

Figure 13: Probabilistic worst-case performance analysis in statistics meaning

5. CONCLUSIONS

This article focuses on developing a general and systematic control methodology for robust active vibration control of piezoelectric flexible structures by building a bridge among several techniques from various disciplines. The proposed control methodology can investigate the effects of structural properties on the natural frequencies and consider them in various robustness analysis to quantitatively verify the robustness properties of the closed-loop system both in the deterministic sense and the probabilistic one. The proposed control methodology can reduce the conservatism in classical robust control from a practical point of view. In this article, the design process and the effectiveness of the proposed control methodology are illustrated by active vibration control of a piezoelectric cantilever beam. In the following research, the proposed methodology may be applied to other structures in the presence of various uncertainties, *e.g.* (Zhong et al., 2010), and be applied to multiple-input and multiple-output (MIMO) systems. Based on (Dinh et al., 2005) it can also be extended to handle time-varying uncertainties.

References

Balas, G., Doyle, J., 1994. Robustness and performance trade-offs in control design for flexible structures. IEEE Transactions on Control Systems Technology 2 (4), 352–361.

Balas, M., 1978a. Active control of flexible systems. Journal of Optimization Theory and Applications 25 (3), 415–436.

Balas, M., 1978b. Feedback control of flexible systems. IEEE Transactions on Automatic Control 23 (4), 673–679.

Balas, M., 1979. Direct velocity feedback control of large space structures. Journal of Guidance, Control, and Dynamics 2 (3), 252–253.

Bayon de Noyer, M., Hanagud, S., 1998. Single actuator and multi-mode acceleration feedback control. Journal of Intelligent Material Systems and Structures 9 (7), 522–533.

Braatz, P., Young, P., Doyle, J., Morari, M., 1994. Computational complexity of μ calculation. IEEE Transactions on Automatic Control 39 (5), 1000–1002.

Calafiore, G., Dabbene, F., Tempo, R., 2000. Randomized algorithms for probabilistic robustness with real and complex structured uncertainty. IEEE Transactions on Automatic Control 45, 2218–2235.

Choi, S., Grandhi, R., Canfield, R., Pettit, C., 2004. Polynomial chaos expansion with latin hypercube sampling for estimating response variability. AIAA Journal 42 (6), 1191–1198.

Demetriou, A., Grigoriadis, K., Sweeney, R., 2009. Collocated H_∞ control of a cantilevered beam using an analytical upper-bound approach. Journal of Intelligent Material Systems and Structures 20 (7), 865–873.

Desoer, C., Vidyasagar, M., 1975. Feedback systems: input-output properties. New York: Academic.

Dinh, M., Scorletti, G., Fromion, V., Magarotto, E., 2005. Parameter dependent H_∞ control by finite dimensional LMI optimization: application to trade-off dependent control. International Journal of Robust and Nonlinear Control 15 (9), 383–406.

Dong, X., Meng, G., Peng, J., 2006. Vibration control of piezoelectric smart structures based on system identification technique: Numerical simulation and experimental study. Journal of Sound and Vibration 297, 680–693.

Duong, P., Lee, M., 2010. Multi-model PID controller design: Polynomial chaos approach. In: International Conference on Control Automation and Systems (ICCAS). pp. 690–695.

Ferreres, G., Biannic, J., Magni, J., 2003. Robustness analysis of flexible structures: practical algorithms. International Journal of Robust and Nonlinear Control 13 (8), 715–733.

Ferreres, G., Biannic, J., Magni, J., 2004. A skew mu toolbox (SMT) for robustness analysis. In: IEEE International Symposium on Computer Aided Control Systems Design. pp. 309–314.

Ferreres, G., Fromion, V., 1999. A new upper bound for the skewed structured singular value. International Journal of Robust and Nonlinear Control 9 (1), 33–49.

Fisher, J., Bhattacharya, R., 2009. Linear quadratic regulation of systems with stochastic parameter uncertainties. Automatica 45 (12), 2831–2841.

Freudenberg, J., Morton, B., 1992. Robust control of a booster vehicle using H_∞ and SSV techniques. In: Proceedings of the 31st IEEE Conference on Decision and Control. Vol. 2. pp. 2448–2453.

Friswell, M., Inman, D., Rietz, R., 1997. Active damping of thermally induced vibrations. Journal of Intelligent Material Systems and Structures 8 (8), 678–685.

Garcia, E., Dosch, J., Inman, D., 1992. The application of smart structures to the vibration suppression problem. Journal of Intelligent Material Systems and Structures 3 (4), 659–667.

Ghanem, R., Spanos, P., 1991. Stochastic Finite Elements: A Spectral Approach. Springer Verlag, New York.

Hou, T., Luo, W., Rozovskii, B., Zhou, H., 2006. Wiener chaos expansions and numerical solutions of randomly forced equations of fluid mechanics. Journal of Computational Physics 216 (2), 687–706.

Iorga, L., Baruh, H., Ursu, I., 2009. H_∞ control with μ-analysis of a piezoelectric actuated plate. Journal of Vibration and Control 15 (8), 1143–1171.

Jemai, B., Ichchou, M., Jézéquel, L., Noe, M., 1999. An assembled plate active control damping set-up: optimization and control. Journal of Sound and Vibration 225 (2), 327–343.

Jiang, J., Li, D., 2011. Decentralized robust vibration control of smart structures with parameter uncertainties. Journal of Intelligent Material Systems and Structures 22 (2), 137–147.

Khalil, H., 1996. Nonlinear Systems, 2nd Edition. Prentice-Hall New Jersey.

Kishor, D., Ganguli, R., Gopalakrishnan, S., 2011. Uncertainty analysis of vibrational frequencies of an incompressible liquid in a rectangular tank with and without a baffle using polynomial chaos expansion. Acta Mech 220 (0), 257–273.

Liu, J., 2008. Monte Carlo strategies in scientific computing. Springer.

Manan, A., Cooper, J., March 2010. Prediction of uncertain frequency response function bounds using polynomial chaos expansion. Journal of Sound and Vibration 329, 3348–3358.

Moheimani, S., Vautier, B., 2005. Resonant control of structural vibration using charge-driven piezoelectric actuators. IEEE Transactions on Control Systems Technology 13 (6), 1021–1035.

Piefort, V., 2001. Finite element modelling of piezoelectric active structures. Ph.D. thesis, Universite Libre de Bruxelles.

Qiu, J., Tani, J., 1995. Vibration control of a cylindrical shell using distributed piezoelectric sensors and actuators. Journal of Intelligent Material Systems and Structures 6 (4), 474–481.

Qiu, Z., Han, J., Zhang, X., Wang, Y., Wu, Z., 2009. Active vibration control of a flexible beam using a non-collocated acceleration sensor and piezoelectric patch actuator. Journal of Sound and Vibration 326 (3), 438–455.

Schoukens, J., Pintelon, R., 1991. Identification of Linear Systems, A Pratical Guide to Accurate Modeling. Pergamon Press, New York.

Skogestad, S., Postlethwaite, I., 2005. Multivariable Feedback Control: Analysis and Design. John Wiley and Sons.

Smith, A., Monti, A., Ponci, F., 2006. Robust controller using polynomial chaos theory. In: Conference Record of the 2006 IEEE, Industry Applications Conference, 41st IAS Annual Meeting. Vol. 5. pp. 2511–2517.

Templeton, B., Ahmadian, M., Southward, S., 2012. Probabilistic control using H_2 control design and polynomial chaos: Experimental design, analysis, and results. Probabilistic Engineering Mechanics 30, 9–19.

Tempo, R., Bai, E., Dabbene, F., 1997. Probabilistic robustness analysis: Explicit bounds for the minimum number of samples. Systems & Control Letters 30 (5), 237–242.

Tempo, R., Calafiore, G., Dabbene, F., 2004. Randomized Algorithms for Analysis and Control of Uncertain Systems. Communications and Control Engineering Series. Springer Verlag, London.

Tzou, H., Tseng, C., 1990. Distributed piezoelectric sensor/actuator design for dynamic measurement/control of distributed parameter systems: a piezoelectric finite element approach. Journal of Sound and Vibration 138 (1), 17–34.

Xiu, D., Karniadakis, G., 2002. The wiener-askey polynomial chaos for stochastic differential equations. SIAM Journal on Scientific Computing 24 (2), 619–644.

Young, P., Dolye, J., 1990. Computation of μ with real and complex uncertainties. In: Proceedings of the 29th Conference on Decirion and Control. pp. 1230–1235.

Young, P., Newlin, M., Doyle, J., 1992. Practical computation of the mixed μ problem. In: Proceedings of the American Control Conference. Chicago, pp. 2190–2194.

Zhang, K., Scorletti, G., Ichchou, M., Mieyeville, F., 2012. Phase and gain control policies for robust active vibration control of flexible structures using smart materials, submitted to Smart Materials and Structures.

Zhang, W., Qiu, J., Tani, J., 2004. Robust vibration control of a plate using self-sensing actuators of piezoelectric patches. Journal of Intelligent Material Systems and Structures 15, 923–931.

Zhong, X., Ichchou, M., Gillot, F., Saidi, A., 2010. A dynamic-reliable multiple model adaptive controller for active vehicle suspension under uncertainties. Smart Materials and Structures 19 (045007).

Zhou, K., Doyle, J., Glover, K., 1996. Robust and Optimal Control. Prentice, Hall Upper Saddle River, NJ.